Wave chaos in rapidly rotating stars

François Lignières[1,*] and Bertrand Georgeot[2]
[1]*Laboratoire d'Astrophysique de Toulouse-Tarbes, Université de Toulouse, CNRS, 31400 Toulouse, France*
[2]*Laboratoire de Physique Théorique, Université de Toulouse, UPS, CNRS, 31062 Toulouse, France*
(Received 3 October 2007; published 31 July 2008)

The effects of rapid stellar rotation on acoustic oscillation modes are poorly understood. We study the dynamics of acoustic rays in rotating polytropic stars and show using quantum chaos concepts that the eigenfrequency spectrum is a superposition of regular frequency patterns and an irregular frequency subset respectively associated with near-integrable and chaotic phase space regions. This opens fresh perspectives for rapidly rotating star seismology and also provides a potentially observable manifestation of wave chaos in a large-scale natural system.

DOI: 10.1103/PhysRevE.78.016215 PACS number(s): 05.45.Mt, 97.10.Sj, 97.10.Kc

Since helioseismology revolutionized our knowledge of the Sun's interior, many efforts, including space missions (MOST, COROT, and KEPLER), have been undertaken to detect oscillation frequencies in a large variety of stars [1,2]. But to access the information contained in these data, the observed frequencies must be first associated with the right stellar oscillation modes. This crucial identification process requires a full understanding of the properties of the oscillation spectrum and, for slowly rotating stars like the Sun, the asymptotic theory of high-frequency acoustic modes provided such an understanding [1]. Both the approximate treatment of the centrifugal distortion [3] and the lack of asymptotic theory have so far hindered reliable identification in rapidly rotating pulsators. This long-standing problem mainly concerns massive and intermediate-mass stars [4] like the δ Scuti star Altaïr, whose surface oblateness has been measured by interferometry [5]. Accurate computations of acoustic modes fully taking into account the effect of rotation on the oscillations have only recently been performed for polytropic models of rotating stars [6]. Here we construct the dynamics of acoustic rays to understand the properties of the frequency spectrum.

The acoustic ray model is analogous to the geometrical optics limit of electromagnetic waves or the classical limit of quantum mechanics. The construction of eigenmodes from stellar acoustic rays has already been considered in the integrable case of a nonrotating spherically symmetric star [7]. However, when the ray dynamics is no longer integrable, the problem is known to become of a deeply different nature. This issue has been mostly investigated by the quantum chaos community in the context of the classical limit of quantum systems [8] and the developed concepts have been applied to other wave phenomena such as those observed in, e.g., microwave resonators [9], lasing cavities [10], quartz blocks [11], and underwater waves [12]. The potential interest for stellar seismology has been suggested [13] but not yet demonstrated.

Our star model is a self-gravitating uniformly rotating monatomic perfect gas ($\Gamma=5/3$) where pressure and density follow a polytropic relation $P_e \propto \rho_e^{1+1/N}$ with $N=3$. Neglecting the Coriolis force and the gravitational potential perturbations, small-amplitude adiabatic perturbations around this equilibrium verify

$$\partial_t \rho + \boldsymbol{\nabla}\cdot(\rho_e \mathbf{v}) = 0, \quad \partial_t \mathbf{v} = -\frac{\boldsymbol{\nabla} P}{\rho_e} + \frac{\rho}{\rho_e}\mathbf{g}_e, \quad dP = c_s^2 d\rho, \tag{1}$$

where the density ρ, pressure P, and velocity $\mathbf{v}$ describe the perturbation, while c_s is the sound velocity and $\mathbf{g}_e$ is the effective gravity resulting from the gravitational and centrifugal potentials. As other quantities characterizing the star model, c_s and $\mathbf{g}_e$ vary in the meridian plane of the rotating star. Neglecting gravity waves, these equations can be reduced to the form $(\omega_c^2-\omega^2)\Phi - c_s^2\Delta\Phi = 0$ where $\Phi = \hat{P}/c_s^3$ is related to the time-harmonic pressure perturbation $P = \mathrm{Re}[\hat{P}\exp(-i\omega t)]$ and $\omega_c = \sqrt{(15/64)(\mathbf{g}_e/c_s)^2 + (3/8)\boldsymbol{\nabla}\cdot\mathbf{g}_e}$ is the cutoff frequency whose sharp increase in the outermost layers of the star provokes the back reflection of acoustic waves. The WKB approximation then leads to the eikonal equation $\omega^2 = c_s^2\mathbf{k}^2 + \omega_c^2$. The acoustic ray is the trajectory tangent to the wave vector $\mathbf{k}$ at the point $\mathbf{x}$ and its evolution can be described by Hamilton's equations, $H = \sqrt{c_s^2\mathbf{k}^2 + \omega_c^2}$ being the Hamiltonian [7]. Rays heading toward the star center tend to be refracted by increasing sound velocity while close to the surface nonspecular reflection takes place at $\omega_c = \omega$. As rotation increases, the isocontours of c_s and ω_c are distorted together with the star surface. In the following, we restrict ourselves to axisymmetric modes $L_z = 0$, thus reducing the phase space to four dimensions.

The acoustic ray dynamics has been investigated by integrating numerically the Hamilton's equations and the resulting dynamics is visualized using the standard tool of the Poincaré surface of section (PSS). As rays do not reach the star boundary, the PSS is defined by $r_p(\theta) = r_s(\theta) - d$, where the distance $d = 0.08 r_s(\pi/2)$ from the star surface $r_s(\theta)$ has been chosen such that all but a few whispering gallery rays cross the PSS (only outgoing rays are taken). The two coordinates of the PSS are θ, the colatitude, and k_θ/ω, k_θ being the angular component of $\mathbf{k}$ in the natural basis associated with the coordinate system $[\zeta = r_s(\theta) - r, \theta]$. We use the scaled variable k_θ/ω as, in the limit $\omega \gg \omega_c$, the ray dynamics be-

*ligniere@ast.obs-mip.fr

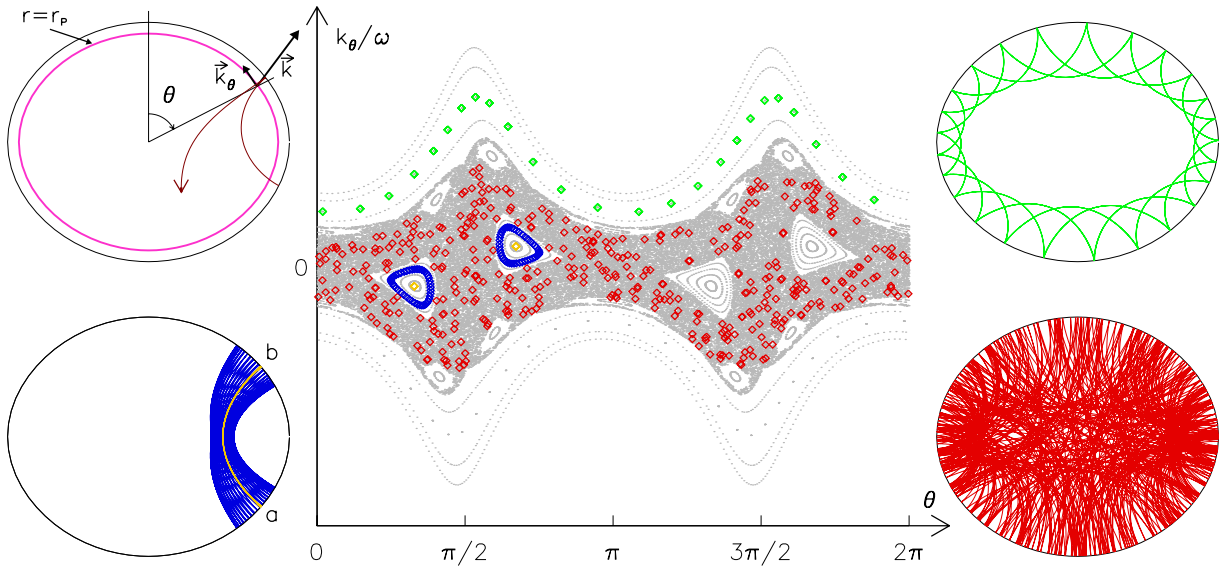

FIG. 1. (Color online) PSS and typical acoustic rays at a rotation equal to 59% of the Keplerian limit. A whispering gallery ray [green (light gray)], an island ray [blue (dark gray)], and a chaotic ray [red (gray)] are shown on the physical space and on the PSS (diamonds in the center figure). The central orbit of the island is also shown (yellow between points a and b). k_θ/ω is in units of $\sqrt{r_s^3(0)/GM}$ with M the stellar mass and G the gravitational constant.

comes independent of the frequency away from the reflection points. We found that increasing the stellar rotation leads to a soft transition from integrability to chaos analogous to the one described by the Kolmogorov-Arnold-Moser (KAM) theorem. As illustrated in Fig. 1 for a given rotation rate, the phase space shows a mixed structure where chaotic regions coexist with a whispering gallery region close to the boundary and regular islands around stable periodic orbits. As the rotation increases, both the chaotic region and the central island chain get larger. A crucial feature of the dynamics is that each region is dynamically isolated from the other by invariant tori which prevent communication between them. Such a situation has been found several times in the domain of quantum chaos, and generally it was surmised [14] that the stationary waves localized on one of these regions form an independent subset with specific dynamical properties. The frequency spectrum thus appears as the superposition of independent frequency subsets reflecting the phase space structure. This surmise has been found to be a good approximation for many systems, although some correlations may remain between the frequency subsets due to modes localized at the border between zones or the presence of partial barriers in phase space [15].

It is therefore important to know if this spectrum organization is valid in the high-frequency limit where it is supposed to hold, and even more important to assess if it is still relevant to the observable acoustic modes. We have thus numerically computed exact axisymmetric modes of Eq. (1), using the method described in [6], in the frequency range $[\omega_1, 12\omega_1]$, ω_1 being the lowest acoustic frequency. To establish a link with the asymptotic ray dynamics, we use a phase-space representation of the modes known as the Husimi distribution [16]. In order to compare a three-dimensional mode with the acoustic rays on a two-dimensional plane, the mode amplitude is first scaled by the square root of the distance to the rotation axis [7]. The Husimi distribution is then constructed from a cut taken along the PSS: $H(s_0,k_0) = |\int \Phi'(s)\exp[-(s-s_0)^2/(2\Delta^2)]\exp(ik_0 s)ds|^2$. Here Φ' is the scaled version of Φ, the integral is taken along the curve $r = r_p$, and k is the moment in the direction tangent to this curve; Δ is the width of the Gaussian wave packet on which Φ' is projected. In Fig. 2, (s_0,k_0) is replaced by (θ,k_θ) for comparison with data from Fig. 1. Except for some of the largest-length-scale modes close to the frequency ω_1, we find that the Husimi distribution enables us to unambiguously associate the modes with the main structures of phase space. As illustrated in Fig. 2, we distinguished the island modes trapped in the main stable islands, the chaotic modes localized in the central chaotic region, and the whispering gallery modes associated with the whispering gallery region. We note that, due to the relatively low frequency considered, the chaotic modes do not spread over all parts of the chaotic region.

Having defined subsets of modes, we can now analyze the properties of the corresponding frequency subsets. As shown in Fig. 3, the frequency spacings of the island modes display striking regularities which lead to the simple empirical formula

$$\omega_{n\ell} = n\delta_n + \ell\delta_\ell + \alpha, \tag{2}$$

where n and ℓ are natural integers, and δ_n and δ_ℓ are uniform frequency spacings. The α constant being fixed by a given island mode frequency, the formula proves sufficiently accurate to identify the other island modes among the whole set of computed frequencies. The phase space representation of these modes reveals that these regular patterns can be attributed to the existence of the stable island region in phase space. Although a zoom on this region would show a complex structure involving chaotic trajectories and chains of small islands nested between deformed surviving tori, these

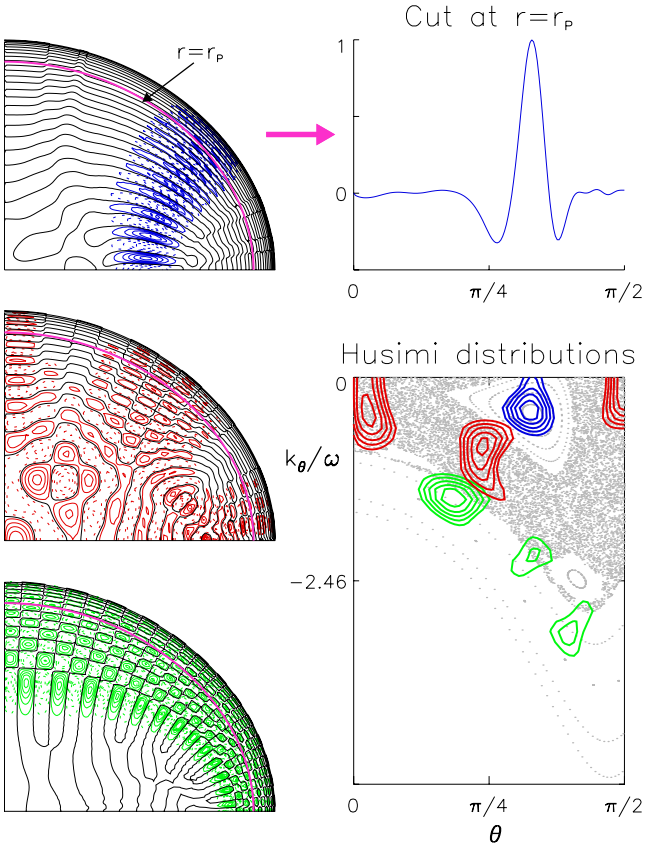

FIG. 2. (Color online) Comparison of numerically computed acoustic modes from (1) with phase space ray dynamics on the PSS. Three typical modes have been selected: island mode [blue (dark gray)], chaotic mode [red (gray)], and whispering gallery mode [green (light gray)]. Left: Spatial distribution of Φ' on one-quarter of a meridian plane. Black lines are the nodal lines, full (dashed) colored (gray) lines are the level curves for positive (negative) values. Magenta line at $r=r_p$ is the chosen PSS. Right top: Cut of the island mode along the PSS, from the pole to the equator. Right bottom: Level curves of the Husimi distributions of the three modes [for the same of value of $\Delta=0.12r_s(\pi/2)$], showing that they are mainly concentrated inside the main stable island (for the island mode), in the chaotic region (for the chaotic mode), or in the whispering gallery region (for the whispering gallery mode).

small-scale details can be overlooked for the relatively large wavelengths considered here. To retrieve formula (2) and to find out how δ_n and δ_ℓ relate to the properties of the star, we follow an approach inspired by the quantization of laser modes in cavities [17]. Indeed, far from the boundary, our problem can be translated into the propagation of light in an inhomogeneous medium, $1/c_s$ playing the role of the medium index. Close to the stable orbit, we can apply the paraxial approximation. In this case, it is known that the wave beam solution is [18] $\Phi(\sigma,\xi)\propto H_\ell[\sqrt{2}\xi/w(\sigma)]\exp[-\xi^2/w(\sigma)^2]\exp[-i\phi(\sigma,\xi)]$, where σ,ξ are coordinates parallel and transverse to the central periodic orbit (the yellow curve in Fig. 1); H_ℓ is the Hermite polynomial of degree ℓ. The spreading of the beam in the transverse direction is described by $w(\sigma)$, which verifies $(1/c_s)d/d\sigma[(1/c_s)(dw/d\sigma)]+\alpha(\sigma)w=4/w^3$, where $\alpha(\sigma)=(1/c_s^3)\partial^2 c_s/\partial\xi^2$. The wave phase is $\phi(\sigma,\xi)=\omega\int_0^\sigma d\sigma'/c_s-2(\ell+1)\int_0^\sigma c_s d\sigma'/w^2+\xi^2/(2c_sR)$ where $R=w/(dw/d\sigma)$ is the radius of curvature of the beam wave front. Numerically computed island modes have a transverse variation confirming this approximation. We then obtain a stationary solution by imposing the requirement that the wave interferes constructively with itself. This requires that the phase accumulated following the periodic orbit ($\xi=0$) from one side of the boundary to the other side is $\omega\int_a^b d\sigma/c_s-2(\ell+1)\int_a^b c_s d\sigma/w^2=n\pi$. This leads to the formula (2) with $\delta_n=\pi/(\int_a^b d\sigma/c_s)$ and $\delta_\ell=2(\int_a^b c_s d\sigma/w^2)/(\int_a^b d\sigma/c_s)$. The numerical value of δ_n obtained from the island mode frequencies shown in Fig. 3 [equal to 0.5514 in units of $\sqrt{GM/r_s^3(0)}$ where M is the stellar mass and G the gravitational constant] is well approximated, within 2.2%, by the theoretical one (equal to 0.5635 in the same units). While δ_n probes the sound velocity along the path of the periodic orbit, δ_ℓ is obtained by solving the second-order equation verified by w together with the two boundary conditions given by the necessity to match R with the radius of curvature of the two bounding surfaces. Thus, δ_ℓ probes the second-order transverse derivative of the sound velocity along the same path as well as the radius of curvature of the bounding surfaces. We note that similar modes around stable periodic orbit have been constructed in other systems, usually with the more systematic procedure of finding the normal forms and using Einstein-Brillouin-Keller quantization [15,19].

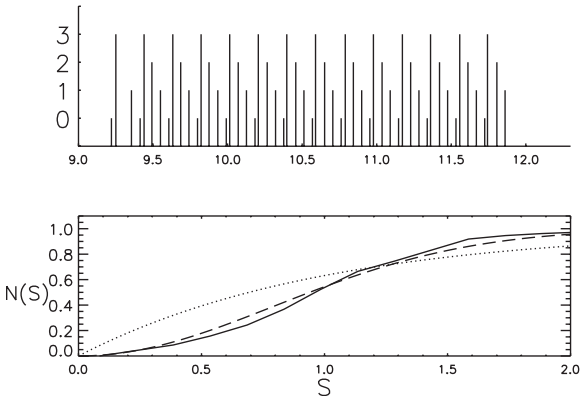

FIG. 3. Top: Island mode frequencies in the interval $[9\omega_1,12\omega_1]$ showing the regular spacings corresponding to formula (2); height reflects the value of the quantum number ℓ. Bottom: Integrated spacing distribution for the chaotic modes in the same interval (full line). Data correspond to around 200 modes from two symmetry classes. The dashed line is the result for the Gaussian orthogonal ensemble of random matrix theory while the dotted line corresponds to the Poisson distribution characteristic of integrable systems.

Having shown that modes whose Husimi distribution is localized in the near-integrable region display integrablelike quantization conditions, we now turn to the modes localized in the chaotic region. The subset of chaotic mode frequencies shows typical signatures of wave chaos such as frequency repulsion. Indeed, in Fig. 3, the integrated distribution of consecutive frequency spacings $S_i=\omega_{i+1}-\omega_i$ (normalized by the mean frequency spacing of those modes) is much closer to the random matrix theory result typical of chaotic systems [20] than to the Poisson distribution result characteristic of

integrable systems. This frequency statistics together with the fact that the corresponding modes are all localized in the chaotic region of the ray dynamics give a strong evidence that wave chaos occurs in rapidly rotating stars. The difficulty of solving Eq. (1) even with state-of-the-art computational techniques prevents us reaching a larger-frequency sample and making detailed comparison with random matrix theory as in, e.g., [20].

The whispering gallery modes and the modes trapped in smaller island chains being associated with near-integrable regions of phase space, their frequencies are therefore expected to display regular patterns. The detail study of these regularities shall be considered elsewhere as it requires more mode calculations with a higher numerical resolution. It is also important to point out that these modes will be the most difficult to detect. Indeed, due to their small latitudinal wavelength (see Fig. 2), the positive and negative light intensity fluctuations strongly cancel out when integrated over the visible disk.

Our results demonstrate that ray dynamics and quantum chaos concepts provide a qualitative and quantitative insight into the frequency spectrum of rapidly rotating stars. In particular, we are able to separate the spectrum of a reasonably realistic star model into integrable and chaotic subsets. Being much less demanding than a direct eigenmode computation as well as easily adaptable to nonaxisymmetric modes (for which regular frequency patterns have also been found numerically [21]) and to more realistic stellar models, ray dynamics will be essential to investigate the asymptotic properties of the oscillation spectrum.

The present analysis opens further perspectives in the seismology of rapidly rotating stars. The observed spectra differ from theoretical ones, as poorly understood mechanisms governing the intrinsic mode amplitude determine the frequencies that are actually detected. In this context, *a priori* information on the structure of the spectrum is crucial in order to identify the observed frequencies with specific stellar oscillation modes. Our results strongly suggest first looking for regular patterns to identify the island modes and to determine seismic observables such as δ_n and δ_ℓ containing information on the star's interior. The remaining chaotic modes are also of special interest for seismology purposes: they are highly sensitive to small changes of the stellar model [22] and, in contrast to nonradial acoustic modes of slowly rotating stars which avoid the star's center, they probe this region, which is crucial for stellar evolution theory. If enough chaotic modes are seen, their mean frequency spacing, which is known to depend on the volume of the chaotic region, will constrain the stellar rotation.

We thank S. Vidal, D. Reese, M. Rieutord, and L. Valdettaro for their help at various stages of this work. We also thank CALMIP ("Calcul en Midi-Pyrénées") for the use of their supercomputer. This work was supported by the Programme National de Physique Stellaire of INSU/CNRS and the SIROCO project of the Agence National de la Recherche.

[1] J. Christensen-Dalsgaard, Rev. Mod. Phys. **74**, 1073 (2002).
[2] A. Gautschy and H. Saio, Annu. Rev. Astron. Astrophys. **33**, 75 (1995); A. Baglin *et al.*, in *Stellar Structure and Habitable Planet Finding*, edited by F. Favata, I. W. Roxburgh, and D. Galadi, ESA Special Publciation 485 (ESA Publications Division, Noordwijk, 2002), pp. 17–24.
[3] M.-J. Goupil *et al.*, in *Delta Scuti and Related Stars*, edited by M. Breger and M. Montgomery, ASP Conf. Ser. No. 210 (Astronomical Society of the Pacific, San Francisco, 2000), pp. 267–284.
[4] D. W. Kurtz, Astrophys. Space Sci. **284**, 29 (2003).
[5] J. D. Monnier *et al.*, Science **317**, 342 (2007); D. L. Buzasi *et al.*, Astrophys. J. **619**, 1072 (2005).
[6] F. Lignières, M. Rieutord, and D. Reese, Astron. Astrophys. **455**, 607 (2006); D. Reese, F. Lignières, and M. Rieutord, *ibid.* **455**, 621 (2006).
[7] D. O. Gough, in *Astrophysical Fluid Dynamics*, edited by J.-P. Zahn and J. Zinn-Justin, Proceedings of the Les Houches Summer School of Theoretical Physics, XLVII (North-Holland, Amsterdam, 1993), pp. 399–559.
[8] *Chaos and Quantum Physics*, edited by M.-J. Giannoni, A. Voros, and J. Zinn-Justin, Proceedings of the Les Houches Summer School of Theoretical Physics, LII (North-Holland, Amsterdam, 1991).
[9] H.-J. Stöckmann and J. Stein, Phys. Rev. Lett. **64**, 2215 (1990).
[10] J. U. Nöckel and A. D. Stone, Nature (London) **385**, 45 (1997).
[11] C. Ellegaard, T. Guhr, K. Lindemann, J. Nygard, and M. Oxborrow, Phys. Rev. Lett. **77**, 4918 (1996).
[12] M. G. Brown *et al.*, J. Acoust. Soc. Am. **113**, 2533 (2003).
[13] J. Perdang, *Seismology of the Sun and the Distant Stars* (Reidel, Dordrecht, 1986), pp. 141–171.
[14] I. C. Percival, J. Phys. B **6**, L229 (1973); M. V. Berry and M. Robnik, J. Phys. A **17**, 2413 (1984).
[15] O. Bohigas, S. Tomsovic, and D. Ullmo, Phys. Rep. **223**, 43 (1993).
[16] S.-J. Chang and K.-J. Shi, Phys. Rev. A **34**, 7 (1986).
[17] H. Kogelnik and T. Li, Appl. Opt. **5**, 1550 (1966).
[18] G. V. Permitin and A. I. Smirnov, Sov. Phys. JETP **82**, 395 (1996); M. Bornatici and O. Maj, Plasma Phys. Controlled Fusion **45**, 707 (2003).
[19] V. F. Lazutkin, *KAM Theory and Semiclassical Approximations to Eigenfunctions* (Springer, Berlin, 1993).
[20] O. Bohigas, M.-J. Giannoni, and C. Schmit, Phys. Rev. Lett. **52**, 1 (1984).
[21] D. Reese, F. Lignières, and M. Rieutord, Astron. Astrophys. **481**, 449 (2008).
[22] R. Schack and C. M. Caves, Phys. Rev. Lett. **71**, 525 (1993); G. Benenti *et al.*, Eur. Phys. J. D **20**, 293 (2002).